

## LETTERS

No Barrier for the Gas-Phase  $C_2H + NH_3$  Reaction

Shaun A. Carl,\* Rehab M. I. Elsamra, Raviraj M. Kulkarni, Hue M. T. Nguyen, and Jozef Peeters

*Department of Chemistry, University of Leuven, Celestijnenlaan 200F, B-3001 Leuven, Belgium**Received: December 8, 2003; In Final Form: February 25, 2004*

The absolute rate constant of the reaction  $C_2H + NH_3 \rightarrow$  products has been experimentally determined over the temperature range 295–765 K at a pressure of 10 Torr (He) and over the pressure range 5–30 Torr at 295 K. The concentration of  $C_2H$  radicals was monitored in real time using the CH chemiluminescence method following their production by pulsed laser photolysis of  $C_2H_2$  at 193 nm in a slow-flow reaction vessel. The pressure-independent rate constant is large and exhibits a pronounced negative temperature dependence:  $k_1(T) = (1.2 \pm 0.2) \times 10^{-11} \exp[(370 \pm 40) \text{ K}/T] \text{ cm}^3 \text{ s}^{-1}$ , both unusual for reaction of a radical with a saturated molecule. This may be rationalized by strong dipole–dipole and dipole – quadrupole interactions, as have been put forward for the isoelectronic  $CN + NH_3$  reaction. The  $C_2H + NH_3$  reaction is somewhat faster than  $CN + NH_3$ , even though ab initio calculations predict the CCH dipole moment to be smaller than that for CN. However the opposite sign of the dipole moment of  $C_2H$  implies an initial HCC- -HNH<sub>2</sub> alignment, favorable for subsequent H-abstraction. The (extrapolated) high rate constant both at combustion temperatures and at interstellar temperatures should make this reaction very important in those environments.

## I. Introduction

Most gas-phase reactions of radicals with closed-shell molecules face sizable energy barriers, and thus have negligible rate constants at the very low temperatures ( $10 \text{ K} \leq T \leq 100 \text{ K}$ ) found in interstellar clouds where the chemistry is dominated by barrier-less reactions governed by long-range attractive forces. Some radical-molecule reactions though do have large rate constants at low temperatures; a notable example being the reaction of the cyano radical with ammonia,  $CN + NH_3$ , with  $k(100 \text{ K}) \approx 1 \times 10^{-10} \text{ cm}^3 \text{ s}^{-1}$ .<sup>1</sup> This large rate constant and its unexpectedly sharp decrease with increasing temperature has been of recent interest to experimentalist and theoreticians.<sup>1–4</sup>

Capture theories<sup>5</sup> that assume the reaction dynamics are controlled by long-range forces and that reaction is guaranteed once over the centrifugal barrier have attempted to reproduce the rate constants of such reactions. For  $CN + NH_3$  there has been limited success: capture theory roughly reproduces the magnitude of the rate constant at low temperatures but the

predicted  $T$  dependence is much too weak. These deficiencies in relation to the  $CN + NH_3$  reaction have been pointed out by Faure et al.<sup>3,4</sup> They have shown that inclusion of ( $NH_3-$ ) quadrupole–(CN) dipole interaction significantly increases the attraction potential at large to midrange internuclear distances but that the temperature dependence is reproduced only by inclusion of rotational selection, in which the reaction is favorable when low-energy rotations are involved. Such theoretical treatments though are still in development.

The isoelectronic counterpart of CN, the ethynyl radical ( $C_2H$ ), is also found in interstellar regions<sup>6–9</sup> and in planetary atmospheres.<sup>10,11</sup> Thus, its low-temperature kinetics too have received attention,<sup>12–17</sup> though the reaction



has not previously been studied either theoretically or experimentally.

At higher temperatures,  $C_2H$  is found as an intermediate in hydrocarbon combustion<sup>18,19</sup> where it is linked to acetylene oxidation and to the formation of polycyclic aromatic hydrocarbons, the precursors of soot.<sup>20–24</sup>  $C_2H$  is also known to be responsible for the intense  $CH(A \rightarrow X)$  chemiluminescence in flames via  $C_2H + O \rightarrow CH(A) + CO$  and  $C_2H + O_2 \rightarrow CH(A) + CO_2$ .<sup>25,26</sup> Finally,  $C_2H$  radicals may take part<sup>27</sup> in “ $NO_x$  reburning”, in which small hydrocarbon radicals, generated from fuel injected above the main combustion zone, reduce  $NO_x$  emissions by rapid reactions with  $NO$  and  $NO_2$  to yield  $HCN$  or  $NCO$ , thus initiating a series of reactions leading to  $N_2$  via  $NH_2$ ,  $NH$ ,  $N$ , and other intermediates.<sup>28–32</sup> This “ $NO_x$  reburning” can be enhanced by injecting  $NH_3$  (“advanced reburning”)<sup>33</sup> into the combustion zone thus generating larger concentrations of  $NH_i$  intermediates. Besides, fuel-bound nitrogen will also give rise to  $NH_3$  in combustion environments.

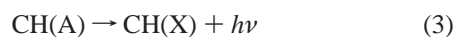
## II. Experimental Section

The pulsed-laser photolysis/chemiluminescence experimental apparatus used in this study is described elsewhere.<sup>34,35</sup> The principal features are given here.  $C_2H$  radicals were generated by pulsed laser photolysis of  $C_2H_2$  at 193 nm in a heatable, blackened, stainless steel reaction cell equipped with windows for passage of the photolysis beam and for chemiluminescence detection at right angles to it. A homogeneous mixture of the excess reactant ( $NH_3$ ), carrier gas (He), and  $C_2H$  precursor ( $C_2H_2$ ) was flowed through the cell at a sufficient rate to refresh the gas between successive photolysis pulses. The gas purities were as follows: He, 99.999%;  $C_2H_2$  (acetone free), 99.6%;  $NH_3$ , 99.96%.  $NH_3$  was diluted in high-purity He to a fraction of about 0.1 before use. For most experiments the total gas pressure was 10 Torr.

Any  $[C_2H(A)]$  formed with  $[C_2H(X)]$  by photolysis of  $C_2H_2$ <sup>36,37</sup> will be quenched rapidly by (10 Torr) helium, at a rate of about  $1.3 \times 10^6 \text{ s}^{-1}$ ,<sup>37</sup> such that only a fraction of less than  $1.5 \times 10^{-3}$  survives after  $5 \mu\text{s}$ , at the inception of the  $C_2H$  decay measurements.

Contrary to some earlier suggestions,<sup>38,40</sup> it has been firmly established recently<sup>41,42</sup> that  $C_2H$  is the only primary photo-product of the 193 nm  $C_2H_2$  dissociation. The low 193 nm laser fluence of ca.  $1.0 \times 10^{16} \text{ photons cm}^{-2}$  per pulse precludes possible two-photon products.<sup>36</sup>

The real-time decay of  $[C_2H]$  was monitored by measuring the intensity of the 431 nm  $CH(A \rightarrow X)$  chemiluminescence resulting from the reaction of  $C_2H$  with  $O_2$  added in large excess.<sup>35</sup> Thus,  $C_2H$  radicals undergo reactions with the co-reactant  $NH_3$ , its precursor  $C_2H_2$ , and  $O_2$ , all in large excess



As the  $CH(A)$  lifetime, of  $\approx 0.5 \mu\text{s}$ ,<sup>39</sup> is less than the chemical lifetime of  $C_2H$  in our experiments, the  $CH(A \rightarrow X)$  emission intensity,  $I_{\text{obs}}(t)$ , is proportional to  $[C_2H]$ , since  $[O_2]$  is constant, such that

$$I_{\text{obs}}(t) \propto [C_2H](t) \propto [C_2H]_0 \exp(-k't) \quad (i)$$

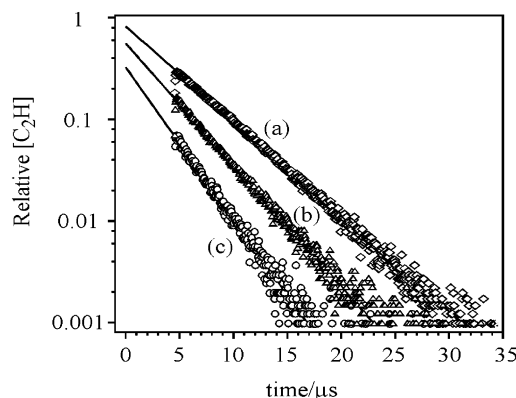


**Figure 1.** Typical time profiles of  $[C_2H]$  following its production by pulsed photodissociation of  $C_2H_2$  at 193 nm in the presence of  $[C_2H_2] = 1.7 \times 10^{15} \text{ cm}^{-3}$ ,  $[O_2] = 1.5 \times 10^{15} \text{ cm}^{-3}$ , temperature of 450 K, and a total pressure of 10 Torr (He): (a)  $[NH_3] = 0.0 \text{ cm}^{-3}$ ; (b)  $[NH_3] = 1.1 \times 10^{15} \text{ cm}^{-3}$ ; (c)  $[NH_3] = 3 \times 10^{15} \text{ cm}^{-3}$ . Each decay is fitted by the expression  $k' = A \exp(-k_{\text{total}}t)$ .

with

$$k' = k_1[NH_3] + k_2[O_2] + k_4[C_2H_2]$$

The  $CH(A \rightarrow X)$  chemiluminescence from the irradiated reaction volume chamber was imaged onto an optically filtered ( $430 \pm 10 \text{ nm}$ ) photomultiplier tube (PMT). The transient signal was digitized and stored on computer. Typically 15 intensity-vs-time profiles were averaged for each  $k'$  measurement. At each single temperature,  $k'$  values were measured for seven to nine different  $[NH_3]$  ranging from 0 to ca.  $7 \times 10^{15} (295 \text{ K/T}) \text{ cm}^{-3}$ , but at a fixed  $[C_2H_2]$  of  $2.5 \times 10^{15} (295 \text{ K/T}) \text{ cm}^{-3}$  and fixed  $[O_2]$  of  $2.3 \times 10^{15} (295 \text{ K/T}) \text{ cm}^{-3}$ . On the basis of a 193 nm absorption cross-section for  $C_2H_2$  of  $1.4 \times 10^{-19} \text{ cm}^2$ <sup>40</sup> and a quantum yield for  $C_2H$  production of unity,<sup>41,42</sup>  $[C_2H]_0$  was calculated to be  $3.5 \times 10^{12} (295 \text{ K/T}) \text{ cm}^{-3}$ , sufficiently small to ensure a negligible influence ( $< 1\%$ ) of any secondary or side ( $C_2H$ -radical) reactions. The absence of any effects from H atoms and  $NH_2$  generated by  $NH_3$  photolysis is discussed below.

The first-order decay rates,  $k'$ , are determined by a weighted least-squares fit to  $I_{\text{obs}}(t)$ , each time after subtraction of an emission transient taken in the absence of  $O_2$  to correct for scattered laser light and window fluorescence.

Since  $k_2'$  and  $k_4'$  are constants for a fixed  $[O_2]$  and  $[C_2H_2]$ , respectively, the term  $k_2[O_2] + k_4[C_2H_2]$  appears only as an ordinate intercept in a plot of  $k'$  vs  $[NH_3]$ , whereas the slope of the resulting straight line equals the bimolecular rate constant  $k_1$ .

## III. Results and Discussion

Figure 1 shows three  $I_{\text{obs}}(t)$   $C_2H$ -decay profiles at 450 K: (a) in the absence of  $NH_3$ , where  $C_2H$  is removed solely by  $O_2$  and  $C_2H_2$ ; (b and c) in the presence of (increasing amounts of)  $NH_3$ , resulting in an increase of the decay rate. All  $I_{\text{obs}}(t)$  profiles exhibit single-exponential behavior over about 2 orders of magnitude. The smaller  $[C_2H]$  at  $t \rightarrow 0$  for increasing  $[NH_3]$  is due to 193 nm absorption by  $NH_3$ . Figure 2 shows plots of  $k'$  as a function of  $[NH_3]$  for three temperatures  $T$ . Linear fits yield  $k_1$  as slope and  $k_2[O_2] + k_4[C_2H_2]$  as intercept.

At the 193 nm  $NH_3$  absorption cross section of  $5.4 \times 10^{-18} \text{ cm}^2$ ,<sup>43</sup> and at our typical 193 nm laser fluences of  $9\text{--}11 \text{ mJ cm}^{-2} \text{ pulse}^{-1}$  a fraction ca. 0.05 of the  $NH_3$  should be photolyzed, generating H and  $NH_2$  at near-unity quantum yield.<sup>43</sup> As the rate constants of the combinations of H and  $NH_2$  with  $C_2H$  at 10 Torr of He may be estimated to be of the order  $5 \times$

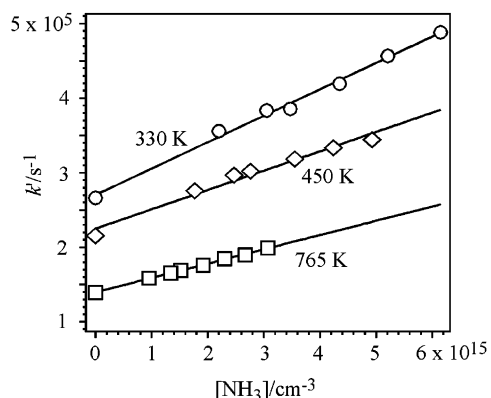


**Figure 2.** Second-order plots of  $k'$  vs  $[\text{NH}_3]$  at three representative temperatures.

**TABLE 1: Derived Experimental Rate Constants for the  $\text{C}_2\text{H} + \text{NH}_3$  Reaction**

$T/\text{K}$	$P/\text{Torr}$	$k'/\text{cm}^3 \text{ s}^{-1}$
295	30	$4.3 \pm 0.6$
295	5.0	$4.2 \pm 0.8$
295	10.0	$4.4 \pm 0.8$
333	10.0	$3.5 \pm 0.6$
350	10.0	$3.0 \pm 0.5$
450	10.0	$2.6 \pm 0.4$
500	10.0	$2.2 \pm 0.4$
650	10.0	$2.2 \pm 0.2$
765	10.0	$1.9 \pm 0.1$

$10^{-11} \text{ cm}^3 \text{ s}^{-1}$ , i.e., close to  $k_1(\text{C}_2\text{H} + \text{NH}_3)$ , the  $k_1$  values from the slopes of  $k'$  vs the *input*- $[\text{NH}_3]$  plots might be systematically 5–10% too high. To test this,  $k_1(295 \text{ K})$  was measured at laser fluences of 4.3 and 11.8  $\text{mJ cm}^{-2}$  per pulse, under the same chemical conditions, yielding  $k_1$  values differing less than 3%. Thus, the combined influence of  $\text{NH}_3$  photolysis with H and  $\text{NH}_2$  generation on the derived  $k_1$  is small and lies within the uncertainty of our determinations. A rationalization is fast recombination of H and  $\text{NH}_2$  at the higher  $[\text{NH}_3]$ ; also, H and/or  $\text{NH}_2$  may react slower than  $\text{NH}_3$  with  $\text{C}_2\text{H}$ . Nonetheless, an additional systematic error of  $\pm 8\%$  was imposed on the derived  $A$  factors on the fits to  $k_1(T)$  vs  $T$ . All  $k_1$  values with their  $2\sigma$  statistical uncertainties are listed in Table 1. Measurements over the pressure range 5–30 Torr of He, also in Table 1, show  $k_1(295 \text{ K})$  to be independent of pressure.

Our  $k_1(T)$  results show that  $\text{C}_2\text{H} + \text{NH}_3$  is unusually fast for a radical + closed-shell-molecule reaction, with  $k_1(295 \text{ K}) = (4.2 \pm 0.6) \times 10^{-11} \text{ cm}^3 \text{ s}^{-1}$ , though it slows down markedly at higher  $T$ . The Arrhenius fit of Figure 3 yields  $k_1(T) = (1.2 \pm 0.2) \times 10^{-11} \exp[(370 \pm 40) \text{ K}/T] \text{ cm}^3 \text{ s}^{-1}$ . A more useful expression for extrapolation to lower  $T$  is  $k_1(T) = (3.9 \pm 0.4) \times 10^{-11} (T/295 \text{ K})^{-0.75 \pm 0.10}$ . Both expressions include statistical ( $2\sigma$ ) and likely systematic errors. Clearly, reaction 1 proceeds without a barrier, similar to  $\text{CN} + \text{NH}_3$ .<sup>1,44</sup> The plot of  $k$  vs  $T$  in Figure 4 shows the similar  $k(T)$  behavior of the two isoelectronic reactions, though  $\text{C}_2\text{H} + \text{NH}_3$  is faster at the lower end of the  $T$ -range of overlap. Most likely, dipole–dipole and dipole–quadrupole interactions, as invoked to reproduce the low- $T$  behavior of  $k(\text{CN} + \text{NH}_3)$ ,<sup>4</sup> are also involved in the fast capture of  $\text{C}_2\text{H}$  by  $\text{NH}_3$ . An important difference, however, is that the dipole moment  $\mu(\text{C}-\text{N}) = +1.70 \text{ D}$ <sup>4</sup> whereas  $\mu(\text{C}-\text{CH}) = -0.77 \text{ D}$ .<sup>45</sup> The lower  $\mu(\text{C}-\text{CH})$  is likely (over-)compensated by its opposite sign which results in an initial  $\text{HCC}^- \cdots \text{H}_3\text{N}$  alignment favorable for an H-abstraction transition structure  $\text{HCC}^- \cdots \text{H}-\text{NH}_2$  – contrary to the CN counterpart. Note that the low- $T$  rate constant should be due

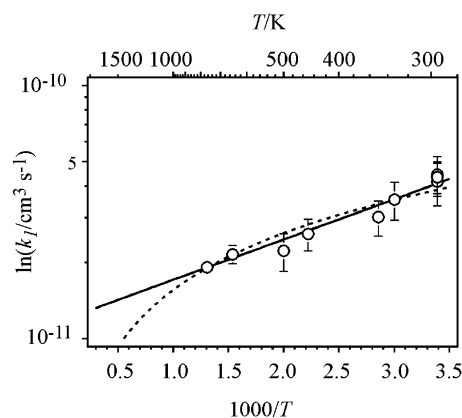


**Figure 3.** Arrhenius plot of the  $\text{C}_2\text{H} + \text{NH}_3$  rate constants. The best fit Arrhenius expression (solid line) is  $k_1(T) = (1.2 \pm 0.2) \times 10^{-11} \exp[(370 \pm 40) \text{ K}/T]$ . The dotted line is a fit to the data of the form  $k_1(T) = A(T/295 \text{ K})^n$ , with  $A = (3.9 \pm 0.4) \times 10^{-11}$  and  $n = -0.75 \pm 0.10$ .

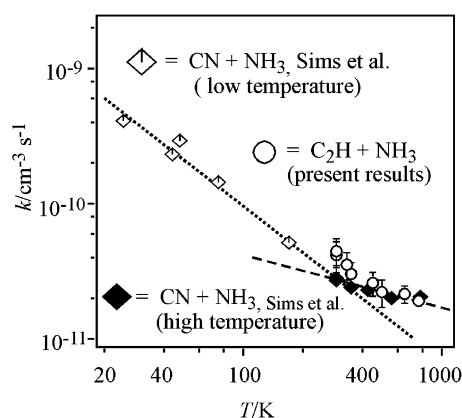


**Figure 4.** Plot of the experimental rate constants for  $\text{C}_2\text{H} + \text{NH}_3$  (open circles) encompassing the low-temperature range over which data for the isoelectronic,  $\text{CN} + \text{NH}_3$ , reaction exists (also plotted). The dotted line shows a fit to the low-temperature experimental data of Sims et al.<sup>1</sup> for  $\text{CN} + \text{NH}_3$  (open diamonds) and the dashed line shows the fit to the high-temperature experimental data of Sims et al.<sup>44</sup> for  $\text{CN} + \text{NH}_3$  (filled triangles).

mostly to slowly rotating reactants as these are more sensitive to the anisotropy of the long-range potential.<sup>4</sup> The product channel in line with the above is  $\text{C}_2\text{H} + \text{NH}_3 \rightarrow \text{C}_2\text{H}_2 + \text{NH}_2$ ,  $\Delta_r H(298 \text{ K}) = -21.7 \text{ kcal/mol}$ .<sup>44</sup> However, more exothermic channels ( $\rightarrow \text{CN} + \text{CH}_4$ ;  $\rightarrow \text{HCN} + \text{CH}_3$ ;  $\rightarrow \text{CH}_3\text{CN} + \text{H}$ ;  $\rightarrow \text{CH}_2\text{CN} + \text{H}_2$ ; ...), although requiring more extensive rearrangements, cannot be excluded. The dominant influence of long-range dipole–dipole and dipole–quadrupole effects on  $k_1(\text{C}_2\text{H} + \text{NH}_3)$  is underscored by the fact that  $k_1(295 \text{ K})$  is a factor ca. 450 higher than expected from an Evans–Polanyi correlation between the rate constant of H-abstraction from R–H by  $\text{C}_2\text{H}$  and the R–H bond energy for *nonpolar* R–H compounds,  $\text{C}_2\text{H}_6$ ,  $\text{CH}_4$ , and  $\text{H}_2$ .<sup>46</sup>

The high rate constant of the title reaction should make it an important process in the interstellar medium, in planetary atmospheres, and in combustion environments. It therefore deserves further experimental and theoretical investigation, aimed, among others, at determining  $k_1$  at lower temperatures, where capture theory is more applicable, and establishing the product distribution.

**Acknowledgment.** The authors are indebted to the Fund for Scientific Research (FWO–Vlaanderen), the KULeuven Re-

search Council (GOA Program and doctoral fellowships) for continuing financial support.

## References and Notes

- (1) Sims, I. R.; Queffelec, J.-L.; Defrance, A.; Rebrion-Rowe, C.; Travers, D.; Bocherel, P.; Rowe, B. R.; Smith, I. W. M. *J. Chem. Phys.* **1994**, *100*, 4229.
- (2) Meads, R. F.; Maclagan, R. G. A. R.; Philips, L. F. *J. Phys. Chem.* **1993**, *97*, 3257 and references therein.
- (3) Faure, A.; Rist, C.; Valiron, P. *Chem. Phys.* **1999**, *241*, 29.
- (4) Faure, A.; Rist, C.; Valiron, P. *Astron. Astrophys.* **1999**, *348*, 972.
- (5) Clary, D. C. *Annu. Rev. Phys. Chem.* **1990**, *41*, 61 and references therein.
- (6) Tucker, K. D.; Kutner, M. L.; Thaddeus, P. *J. Astrophys.* **1974**, *193*, L115.
- (7) Jackson, W. M.; Bao, Y. H.; Urdahl, R. S. *J. Geophys. Res.—Planets* **1991**, *96*, 17569.
- (8) Hasegawa, T. I.; Kwok, S. *Astrophys. J.* **2001**, *562*, 824.
- (9) Markwick, A. J.; Ilgner, M.; Millar, T. J.; Henning, T. *Astron. Astrophys.* **2002**, *385*, 632.
- (10) Strobel, D. F. *Planet. Space Sci.* **1982**, *30*, 839.
- (11) Allen, M.; Yung, Y. L.; Gladstone, G. R. *Icarus* **1992**, *100*, 527.
- (12) Pedersen, J. O. P.; Opansky, B. J.; Leone, S. R. *J. Phys. Chem.* **1993**, *97*, 6822.
- (13) Hoobler, R. J.; Leone, S. R. *J. Phys. Chem. A* **1999**, *103*, 1342.
- (14) Lee, S.; Leone, S. R. *Chem. Phys. Lett.* **2000**, *329*, 443.
- (15) Stahl, F.; Schleyer, P. V.; Bettinger, H. F.; Kaiser, R. I.; Lee, Y. T.; Schaefer, H. F. *J. Chem. Phys.* **2001**, *114*, 3476.
- (16) Carty, D.; Le Page, V.; Sims, I. R.; Smith, I. W. M. *Chem. Phys. Lett.* **2001**, *344*, 310.
- (17) Vakhtin, A. B.; Heard, D. E.; Smith, I. W. M.; Leone, S. R. *Chem. Phys. Lett.* **2001**, *348*, 21.
- (18) Shaub, W. M.; Bauer, S. H. *Combust. Flame* **1978**, *32*, 35.
- (19) Peeters, J.; Devriendt, K. *Symp. (Int.) Combust. [Proc.]* **1996**, *26*, 1001.
- (20) Peeters, J. *Bull. Soc. Chim. Belg.* **1997**, *106*, 337.
- (21) Miller, J. A.; Melius, C. F. *Combust. Flame* **1992**, *91*, 21.
- (22) Lindstedt, R. P.; Skevis, G. *Proc. Combust. Inst.* **1996**, *26*, 703.
- (23) Marinov, N. M.; Castaldi, M. J.; Melius, C. F.; Tsang, W. *Combust. Sci. Technol.* **1997**, *128*, 295.
- (24) Moskaleva, L. V.; Mebel, A. M.; Lin, M. C. *Proc. Combust. Inst.* **1996**, *26*, 521.
- (25) Devriendt, K.; Van Look, H.; Ceursters, B.; Peeters, J. *Chem. Phys. Lett.* **1996**, *261*, 450 and references therein.
- (26) Devriendt, K.; Peeters, J. *J. Phys. Chem. A* **1997**, *101*, 2546.
- (27) Peeters, J.; VanLook, H.; Ceursters, B. *J. Phys. Chem.* **1996**, *100*, 15124.
- (28) Bowman, C. T. *Symp. (Int.) Combust. [Proc.]* **1992**, *24*, 859.
- (29) Glarborg, P.; Alzueta, M. U.; Dam-Johansen, K.; Miller, J. A. *Combust. Flame* **1998**, *115*, 1.
- (30) Dagaut, P.; Luche, J.; Cathonnet, M. *Int. J. Chem. Kinet.* **2000**, *32*, 365.
- (31) Carl, S. A.; Sun, Q.; Vereecken, L.; Peeters, J. *J. Phys. Chem. A* **2002**, *106*, 12242.
- (32) Carl, S. A.; Sun, Q.; Teugels, L.; Peeters, J. *Phys. Chem. Chem. Phys.* **2003**, *5*, 5424.
- (33) Xu, X.; Smoot, L. D.; Hill, S. C. *Energy Fuels* **1999**, *13*, 411 and references therein.
- (34) Peeters, J.; Van Hoeymissen, J.; Vanhaelemeersch, S.; Vermeylen, D. *J. Phys. Chem.* **1992**, *96*, 1257.
- (35) Van Look, H.; Peeters, J. *J. Phys. Chem.* **1995**, *99*, 16284.
- (36) Wodtke, A. M.; Lee, Y. T. *J. Phys. Chem.* **1985**, *89*, 4744.
- (37) Shokoohi, F.; Watson, T. A.; Reisler, H.; Kong, F.; Renlund, A. M.; Wittig, C. *J. Phys. Chem.* **1986**, *90*, 5695.
- (38) Laufer, A. H.; Yung, Y. L. *J. Phys. Chem.* **1993**, *87*, 181 and references therein.
- (39) Luque, J.; Crosley, D. R. *Appl. Phys. B: Laser Opt.: Lasers Opt.* **1996**, *63*, 91.
- (40) Seki, K.; Okabe, K. *J. Phys. Chem.* **1993**, *97*, 5284 and references therein.
- (41) (a) Mordaunt, D. H.; Ashford, M. N. R.; Dixon, R. N.; Löffler, P.; Schnieder, L.; Welge, K.-H. *J. Chem. Phys.* **1998**, *108*, 519. (b) Hashimoto, N.; Yonekura, N.; Suzuki, T. *Chem. Phys. Lett.* **1997**, *264*, 545.
- (42) Lauter, A.; Lee, K. S.; Jung, K. H.; Vatsa, R. K.; Mittal, J. P.; Volpp, H. R. *Chem. Phys. Lett.* **2002**, *358*, 314.
- (43) Kenner, R. D.; Rohrer, F.; Stuhl, F. *J. Chem. Phys.* **1987**, *86*, 2036.
- (44) Sims, I. R.; Smith, I. W. M. *J. Chem. Soc., Faraday Trans. 2* **1988**, *84*, 527.
- (45) Flores, J. R.; Estévez, C. M.; Carballeira, L.; Perez Juste, I. *J. Phys. Chem. A* **2001**, *105*, 4716.
- (46)  $k(\text{C}_2\text{H} + \text{C}_2\text{H}_6) = 7.8 \times 10^{-12} \text{ cm}^3 \text{ s}^{-1}$  per abstractable H at 295 K (Ceusters, B.; Nguyen, H. M. Y.; Nguyen, M. T.; Peeters, J.; Vereecken, L. *Phys. Chem. Chem. Phys.* **2000**, *3*, 3070), and the  $\text{H}_3\text{CC}-\text{H}$  bond strength is  $422.8 \pm 1.5 \text{ kJ mol}^{-1}$ ,  $k(\text{C}_2\text{H} + \text{CH}_4) = 7.28 \times 10^{-13} \text{ cm}^3 \text{ s}^{-1}$  per abstractable H at 298 K (Ceursters, B.; Nguyen, H. M. T.; Peeters, J.; Nguyen, M. T. *Chem. Phys. Lett.* **2000**, *329*, 412); the  $\text{H}_3\text{C}-\text{H}$  bond strength is  $438.5 \pm 1.5 \text{ kJ mol}^{-1}$ ,  $k(\text{C}_2\text{H} + \text{H}_2) = 3.5 \times 10^{-13} \text{ cm}^3 \text{ s}^{-1}$  per abstractable H at 295 K (Peeters, J.; Van Look, H.; Ceursters, B. *J. Phys. Chem.* **1996**, *37*, 15125); the H—H bond strength is  $436 \text{ kJ mol}^{-1}$ . The  $\text{H}_2\text{N}-\text{H}$  bond strength is  $449.4 \pm 4.6 \text{ kJ mol}^{-1}$ .